

A Survey on the Envelope Fluctuations of DFT Precoded OFDMA Signals

Tobias Frank, Anja Klein
Technische Universität Darmstadt
FG Kommunikationstechnik
Merckstr. 25
64283 Darmstadt, Germany
Email: t.frank@nt.tu-darmstadt.de

Thomas Haustein
Nokia Siemens Networks GmbH & Co. KG
COO RTP PT Radio System Technology
St.-Martin-Str. 76
81617 München, Germany
Email: thomas.haustein@nsn.com

Abstract—Discrete Fourier Transform (DFT) precoding is a promising approach for reduction of the envelope fluctuations of Orthogonal Frequency Division Multiple Access (OFDMA) signals. However, the envelope fluctuations of DFT precoded OFDMA signals strongly depend on the subcarrier allocation used. In this work, the envelope fluctuations of DFT precoded OFDMA signals with different subcarrier allocations are analyzed based on various metrics. The mutual dependency of the metrics is addressed and a set of suitable metrics for the design of appropriate DFT precoded OFDMA solutions for the uplink of future mobile radio systems is proposed. New results for oversampled signals considering pulse shaping and windowing are presented and analyzed.

I. INTRODUCTION

In future mobile radio systems, Orthogonal Frequency Division Multiplexing (OFDM) and its Multiple Access (MA) derivative Orthogonal Frequency Division Multiple Access (OFDMA) play an important role [1], because they provide many advantages such as high flexibility, good robustness to multipath propagation and low computational complexity for user separation as well as for channel equalization when using a Frequency Domain Equalizer (FDE). However, a major drawback of OFDM and OFDMA are the high envelope fluctuations of the transmit signal [2]. Especially in the uplink, transmit signals with high envelope fluctuations require expensive amplifiers in the mobile terminal and a high power back-off which results in a low power efficiency [3]. Many methods to combat the high envelope fluctuations have been proposed, e.g., at the expense of additional required signalling overhead or increased complexity, cf., e.g., [4]–[7].

Unitary precoding (UP), e.g., using a Discrete Fourier Transform (DFT) is well known to combine the advantages of OFDM(A) with significantly decreased envelope fluctuations, cf. [8], [9]. UP using the DFT does not require any additional signalling and, combined with a regular subcarrier allocation scheme, offers a further reduced computational complexity [10]–[12]. Well known MA schemes based on DFT precoded OFDMA with regular subcarrier allocation are currently proposed as MA solutions for the uplink (UL) in future mobile radio systems. DFT precoded OFDMA with blockwise subcarriers allocation is known as localized Single Carrier Frequency Division Multiple Access (SC-FDMA) [13] or Localized Frequency Division Multiple Access (LFDMA) [14], respectively, and is proposed in the 3rd Generation Partnership Project (3GPP) for the Long Time Evolution (LTE). DFT precoded OFDMA with regularly interleaved subcarrier allocation is known as distributed SC-FDMA [13] or Interleaved Frequency Division Multiple Access (IFDMA) [10], [11], respectively, and is also

proposed in 3GPP LTE. Throughout this work, the denotations LFDMA and IFDMA are used. Another variant of DFT precoded OFDMA using regularly interleaved blocks of subcarriers is denoted Block-IFDMA (B-IFDMA) [15] and has been recently proposed for non-adaptive UL transmission in the European Union (EU) 4G research project WINNER [1].

In theoretical investigations it has been shown that the different DFT precoded OFDMA schemes provide different properties regarding their envelope fluctuations [14]. Under certain assumptions, especially IFDMA can be shown to provide a perfectly constant envelope using Phase Shift Keying (PSK) [11], whereas for LFDMA this is not possible [14]. However, in practical systems a pulse shaping is required in order to fulfill certain spectral requirements given by regulator authorities which increases the envelope fluctuations of the transmit signal.

The envelope fluctuations of a transmit signal can be regarded and evaluated from different perspectives. A common measure is the Peak-to-Average Power ratio. Another one is the Cubic Metric (CM) [16] which has been recently proposed in 3GPP LTE. Other publications focus on the out-of band radiation [17] or on the performance degradation due to a loss of orthogonality [18] while transferring a signal with fluctuating envelope over a non-linear power amplifier.

In this work, the transmit signals for different DFT precoded OFDMA schemes with regular subcarrier allocation, namely B-IFDMA, IFDMA and LFDMA are analyzed and compared. A novel system model for oversampled and pulse shaped B-IFDMA is given that includes the system models for oversampled and pulse shaped IFDMA and LFDMA as a special case. For the analysis of realistic transmit signals including oversampling, pulse shaping and windowing as well as a realistic model for the high power amplifier, new results using different metrics are presented and compared. The relationship between the different metrics is shown, the suitability of the different metrics is discussed and a set of metrics for the design of appropriate multiple access schemes for UL transmission of future mobile radio systems is proposed. Finally, different realistic pulse shapes for IFDMA and B-IFDMA are discussed compared addressing the trade-off between an efficient use of the spectrum, low out-of-band radiation and low envelope fluctuations of the transmit signal.

The remainder of the paper is organized as follows: In Section II, system models for B-IFDMA, IFDMA and LFDMA are given as special cases of a system model for DFT precoded OFDMA. Section III presents the different metrics that are used for analysis throughout this work. The analysis of the envelope fluctuations of the different schemes and the dependencies of the different metrics is presented in Section IV. In Section V, an appropriate pulse shaping for IFDMA and B-IFDMA is

proposed and Section VI concludes this work.

II. SYSTEM MODEL

In this section, new system models for B-IFDMA, IFDMA and LFDMA with oversampling, pulse shaping and windowing are derived as special cases of a system model for DFT-precoded OFDMA. In the following, all signals are represented by their discrete time equivalents in the complex baseband. Further on, $(\cdot)^T$ denotes the transpose, $(\cdot)^{-1}$ the inverse and $(\cdot)^H$ the Hermitian of a vector or a matrix, respectively.

For a system with K users with user index k , $k = 0, \dots, K - 1$, let

$$\mathbf{d}^{(k)} = (d_0^{(k)}, \dots, d_{Q-1}^{(k)})^T \quad (1)$$

denote a block of Q data symbols $d_q^{(k)}$, $q = 0, \dots, Q - 1$, of user k at symbol rate $1/T_s$. For sake of simplicity, throughout this section it is assumed that the same number Q of subcarriers is assigned to each user. However, note that for IFDMA, LFDMA and B-IFDMA also different numbers of subcarriers may be assigned to each user, e.g., using methods as described in [19]. The data symbols $d_q^{(k)}$ may be taken from the alphabet of a bit mapping scheme like Phase Shift Keying (PSK) or Quadrature Amplitude Modulation (QAM), applied after Forward Error Correction (FEC) coding and bit interleaving. Throughout this paper, it is assumed that the modulation and coding scheme is constant within an OFDM symbol. Let $N = K \cdot Q$ denote the number of subcarriers available in the system. The assignment of the data symbols $d_q^{(k)}$ to a user specific set of Q out of N subcarriers is assumed to be described by an $N \times Q$ subcarrier allocation matrix $\mathbf{M}^{(k)}$. With \mathbf{F}_N^H denoting the matrix representation of an N -point Inverse DFT (IDFT), the DFT-precoded OFDMA signal

$$\bar{\mathbf{x}}^{(k)} = (\bar{x}_0^{(k)}, \dots, \bar{x}_{N-1}^{(k)})^T \quad (2)$$

of user k can be described by N elements $\bar{x}_n^{(k)}$, $n = 0, \dots, N - 1$, at sample rate $1/T_c = K/T_s$ and is given by

$$\bar{\mathbf{x}}^{(k)} = \mathbf{F}_N^H \cdot \mathbf{M}^{(k)} \cdot \mathbf{F}_Q \cdot \mathbf{d}^{(k)}, \quad (3)$$

where \mathbf{F}_Q denotes a Q -point DFT matrix for precoding. In the following, an upsampling and a subsequent pulse shaping is applied to $\bar{\mathbf{x}}^{(k)}$. Upsampling in time domain with an upsampling factor S can be obtained by insertion of S zeros inbetween the N samples of the signal $\bar{\mathbf{x}}^{(k)}$. Thus, the oversampled signal

$$\mathbf{x}^{(k)} = (x_0^{(k)}, \dots, x_{S \cdot N - 1}^{(k)})^T \quad (4)$$

is given by

$$\mathbf{x}^{(k)} = (\bar{x}_0^{(k)}, \underbrace{0, \dots, 0}_{S \text{ zeros}}, \bar{x}_1^{(k)}, 0, \dots, 0, \bar{x}_{N-1}^{(k)}, 0, \dots, 0)^T. \quad (5)$$

For pulse shaping we consider a circular convolution of $\mathbf{x}^{(k)}$ with the vector representation of the pulse shaping filter

$$\mathbf{g} = (g_0, \dots, g_{R-1})^T \quad (6)$$

with samples g_r , $r = 0, \dots, R - 1$ at sampling rate S/T_c , where $R \leq S \cdot N$ denotes the length of the filter. Note that circular convolution in time domain corresponds to a forming of the spectrum in the DFT domain. The pulse shaped signal is given by

$$\mathbf{x}_{\text{PS}}^{(k)} = \mathbf{x}^{(k)} \circledast \mathbf{g}, \quad (7)$$

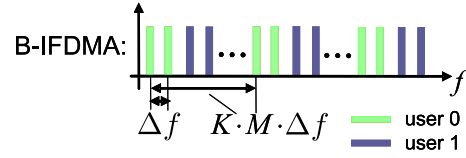


Fig. 1: Illustration of the spectrum of a B-IFDMA signal with subcarrier spacing $\Delta f = N/T_c$.

where \circledast denotes circular convolution. Subsequently, a cyclic prefix (CP) is inserted. The oversampled signal $\tilde{\mathbf{x}}^{(k)} = (\tilde{x}_0^{(k)}, \dots, \tilde{x}_{P+S \cdot N-1}^{(k)})^T$ after insertion of a CP with $P + S \cdot N$ elements at sample rate S/T_c , where P denotes the length of the CP, can be described by

$$\tilde{\mathbf{x}}^{(k)} = (\mathbf{x}_{\text{CP}}^{(k)} \ \mathbf{x}_{\text{PS}}^{(k)})^T, \quad (8)$$

where

$$\mathbf{x}_{\text{CP}}^{(k)} = (x_{\text{PS}, S \cdot N - P}^{(k)}, \dots, x_{\text{PS}, S \cdot N - 1}^{(k)})^T. \quad (9)$$

In order to form the spectrum of the signal, an additional windowing might be applied. Let

$$\mathbf{w} = (w_0, \dots, w_{P+S \cdot N-1})^T \quad (10)$$

denote the vector representation of a time domain window with elements w_s at sampling rate S/T_c . The oversampled DFT-precoded OFDMA signal with CP after windowing

$$\tilde{\mathbf{x}}_{\text{w}}^{(k)} = (\tilde{x}_{\text{w}, 0}^{(k)}, \dots, \tilde{x}_{\text{w}, P+S \cdot N-1}^{(k)})^T \quad (11)$$

is given by

$$\tilde{\mathbf{x}}_{\text{w}}^{(k)} = \mathbf{W} \cdot \tilde{\mathbf{x}}^{(k)}, \quad (12)$$

where \mathbf{W} denotes an $(P + SN) \times (P + SN)$ diagonal matrix carrying the elements w_s ; $s = 0, \dots, P + S \cdot N - 1$ of vector \mathbf{w} on its main diagonal given by

$$\mathbf{W} = \text{diag}(\mathbf{w}). \quad (13)$$

A system model for B-IFDMA can be obtained from the generalized system model for DFT-precoded OFDMA by setting $\mathbf{M}^{(k)} = \mathbf{M}_B^{(k)}$, where $\mathbf{M}_B^{(k)}$ denotes a subcarrier allocation matrix for block interleaved allocation. Let L and M denote the number of blocks and the number of subcarriers per block, respectively, with $L \cdot M = Q$. Note, that B-IFDMA can be regarded as a generalization of both, LFDMA and IFDMA. Thus, for $M = 1$ B-IFDMA is equal to LFDMA and for $L = 1$ B-IFDMA is equal to IFDMA. The elements $M_B^{(k)}(n, q)$, in the n -th row, $n = 0, \dots, N - 1$, and q -th column, $q = 0, \dots, Q - 1$, of matrix $\mathbf{M}_B^{(k)}$ are given by

$$M_B^{(k)}(n, q) = \begin{cases} 1 & n = l \cdot \frac{N}{L} + m + kM \\ 0 & \text{else} \end{cases}, \quad (14)$$

where $l = 0, \dots, L - 1$; $m = 0, \dots, M - 1$. An illustration for the spectrum of B-IFDMA showing the signals of 2 users is given in Fig. 1. Oversampling, insertion of the CP and windowing for B-IFDMA is obtained according to (4) - (12).

III. METRICS FOR EVALUATION OF THE ENVELOPE FLUCTUATIONS

Many different metrics have been proposed for the evaluation of the envelope fluctuations of a signal. In the following, a brief overview over those metrics is given that are considered as most important throughout this work. A widely used metric is the Peak-to-Average Power Ratio (PAPR) [20] per OFDM symbol which can be defined as

$$PAPR = \max_s \left\{ \frac{|\tilde{x}_{w,s}^{(k)}|^2}{E\{|\tilde{x}_{w,s}^{(k)}|^2\}} \right\}, \quad s = 0, \dots, P + S \cdot N - 1, \quad (15)$$

where $E\{\cdot\}$ denotes the expectation of a random variable. Defined according to (15), the PAPR gives the ratio of the peak power to the average power within an OFDM symbol. However, dependent on the data symbols, the PAPR varies from OFDM symbol to OFDM symbol. Thus, in order to obtain meaningful results, not only the maximum PAPR but also the probability distribution of the PAPR over many consecutive OFDM symbols is regarded.

Recently, a new metric denoted Cubic Metric (CM) has been receiving wide interest in 3GPP LTE. The CM is based on the fact that the primary cause of distortion is the third order non-linearity of the amplifier gain characteristic [21]. A description of the intensity of the third order non-linearity is given by normalizing the transmit signal $\tilde{x}_w^{(k)}$ to a root mean square (RMS) value equal to one and then calculating the RMS of the cubed normalized signal according to

$$RCM = 20 \log_{10} \left(\text{RMS} \left(\left(\frac{|\tilde{x}_{w,s}^{(k)}|}{\text{RMS}(\tilde{x}_{w,s}^{(k)})} \right)^3 \right) \right), \quad (16)$$

where

$$\text{RMS}(\tilde{x}_{w,s}^{(k)}) = \sqrt{\frac{1}{P + S \cdot N} \sum_{s=0}^{P+S \cdot N - 1} |\tilde{x}_{w,s}^{(k)}|^2} \quad (17)$$

denotes the RMS of the elements $\tilde{x}_{w,s}^{(k)}$ of vector $\tilde{x}_w^{(k)}$. The metric RCM is known as Raw Cubic Metric (RCM) and is often used in comparison to a reference signal with $CM_{ref} = 1.52$ which is the linear RCM of a Wideband Code Division Multiple Access (W-CDMA) signal [16].

Together with a non-linear amplifier, a fluctuating signal envelope results in undesired out-of-band radiation [17]. In order to meet a certain spectral mask of the signal that is usually predefined by regulator authorities, a certain power back-off is required for the amplifier. The higher the required power back-off, the less power efficient the use of the amplifier [17]. Thus, a further metric for evaluation of the envelope fluctuation of a signal is the required amplifier power back-off in order to meet a given spectral mask for a given amplifier model. In the following, the Rapp model [20] is used in order to model the non-linear power amplifier. The output of the amplifier according to the Rapp model is given by

$$\tilde{y}_{w,s}^{(k)} = \frac{\tilde{x}_{w,s}^{(k)}}{\left(1 + \left(\frac{\tilde{x}_{w,s}^{(k)}}{x_{sat}} \right)^{2p} \right)^{\frac{1}{2p}}}, \quad (18)$$

where p denotes the Rapp-Parameter and x_{sat} denotes the saturation level of the amplifier. Large values of p , e.g., $p = 10$,

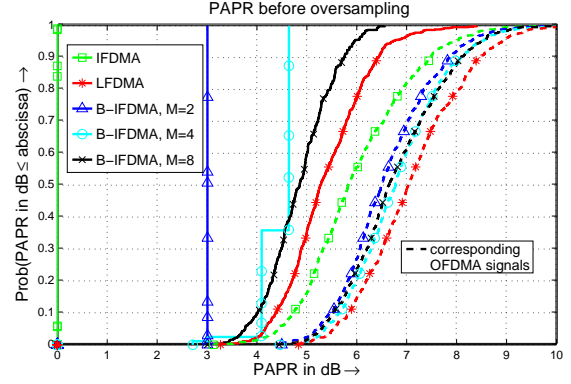


Fig. 2: PAPR for the transmit signal before upsampling of different multiple access schemes for $Q=32$ subcarriers per user and $N=1024$ subcarriers available in the system using QPSK modulation.

model a highly linear amplifier whereas with decreasing values of p the non-linearity of the amplifier increases. The relation between the saturation level x_{sat} , the power P_{in} of the input signal $\tilde{x}_{w,s}^{(k)}$ and the power back-off IBO is given by

$$IBO = 10 \log_{10} \left(\frac{|x_{sat}|^2}{P_{in}} \right). \quad (19)$$

In the following, the power back-off IBO that is required in order to meet a given spectral mask, e.g., according to [22], is regarded for a given amplifier model.

Another important effect of transmitting an OFDMA based signal with fluctuating envelope over a non-linear amplifier is that the orthogonality of the subcarriers is destroyed. Thus, the performance of the received signal degrades with decreasing the power back-off of the amplifier. Consequently, the performance degradation, e.g., in terms of Bit Error Rates (BER) is a further metric in order to evaluate the effect of envelope fluctuations in presence of non-linear amplifiers. In the following, the BER degradation for transmission over an AWGN channel is regarded. The reason to use an AWGN channel for transmission is that the different regarded subcarrier allocations provide different amounts of frequency diversity when transmitted over a frequency selective channel. Performance degradations due to non-orthogonal subcarriers and performance gains due to frequency diversity should be well separated in this analysis.

IV. ANALYSIS OF THE ENVELOPE FLUCTUATIONS

In Figs. 2 and 3, the cumulative distribution function (CDF) of the PAPR is shown for B-FDMA, IFDMA and LFDMA as well as for the corresponding non-DFT precoded OFDMA schemes with the same subcarrier allocation for a signal without oversampling, i.e., $S = 1$. It is well known that in this case the signal processing for IFDMA reduces to a simple compression and repetition of the data symbol vector $\mathbf{d}^{(k)}$ and subsequent user specific phase rotation [10]. Therefore, using PSK, a constant envelope of the signal is provided. For an increasing number of subcarriers per block the PAPR increases and converges to the PAPR for LFDMA, where all subcarriers assigned to a certain user are concentrated in one block. For higher order modulation such as 64QAM, cf. Fig. 3, the PAPR increases for all DFT precoded modulation schemes. However, the relative increase is much more significant for IFDMA than for LFDMA.

In Fig. 4, a signal with oversampling factor $S = 8$ using a Raised Cosine window with a roll-off region that is 5% of the symbol duration is assumed. As pulse shaping filter, an ideal lowpass filter is assumed. Compared to the CDF of the

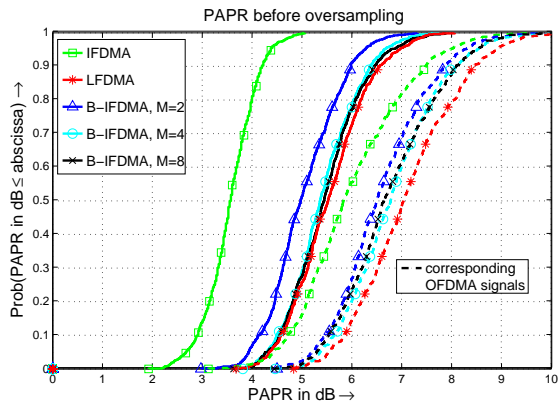


Fig. 3: PAPR for the transmit signal before upsampling of different multiple access schemes for $Q=32$ subcarriers per user and $N=1024$ subcarriers available in the system using 64QAM modulation.

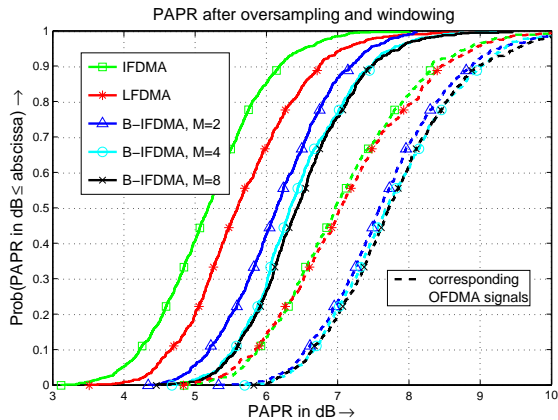


Fig. 4: PAPR for the transmit signal before after upsampling, pulse shaping and windowing of different multiple access schemes for $Q=32$ subcarriers per user and $N=1024$ subcarriers available in the system using QPSK modulation.

PAPR for $S = 1$, for the oversampled and windowed signal the results are different. The advantageous PAPR of IFDMA is lost since the signal cannot be described any longer by compression, repetition and subsequent phase rotation due to the oversampling and the pulse shaping. As a result, the PAPR for IFDMA after oversampling and pulse shaping is similar to the PAPR for LFDMA. However, also for the oversampled and pulse shaped signal, for B-IFDMA the PAPR increases compared to IFDMA and LFDMA with increasing number of subcarriers per block. The reason for that is, that the B-IFDMA time domain signal can be described as a superposition of M signals, cf. [12]. In all cases, the DFT precoded OFDMA schemes show an up to ≈ 1.3 dB lower PAPR compared to the corresponding OFDMA scheme with the same subcarrier allocation. The reason for that is that, according to the definition of the IDFT that is used for OFDM modulation, the OFDMA time domain signal is given by a superposition of Q data symbols, each weighted with a complex exponential, whereas for DFT precoded OFDMA the complex exponentials from the IDFT for OFDM modulation and from the DFT for precoding partially cancel out each other.

In Table I, the average PAPR and the maximum PAPR values are compared to the RCM for the oversampled and windowed signal using the same parameters as for the PAPR results shown in Figs. 2-4. From Table I it can be concluded that RCM and average PAPR lead to the same conclusions although they are different metrics. Using both metrics, in all cases DFT precoded OFDMA results in lower values for the RCM and the average

TABLE I: Simulation results for the Raw Cubic Metric (RCM), the maximum PAPR and the average PAPR for different MA schemes and different modulation schemes. In brackets, the respective metrics for the corresponding non-DFT precoded OFDMA schemes are given.

		RCM	Max. PAPR	Aver. PAPR
B-IFDMA (OFDMA)	QPSK	5.34 (7.82)	9.45 (10.86)	6.49 (7.80)
	16QAM	6.20 (7.83)	9.77 (10.28)	6.87 (7.80)
	M=8 64QAM	6.24 (7.83)	10.06 (10.35)	6.84 (7.81)
B-IFDMA (OFDMA)	QPSK	5.31 (7.83)	9.26 (11.37)	6.43 (7.79)
	16QAM	6.18 (7.83)	9.68 (10.55)	6.84 (7.80)
	M=4 64QAM	6.31 (7.83)	9.24 (11.24)	6.87 (7.80)
B-IFDMA (OFDMA)	QPSK	4.96 (7.77)	8.11 (11.58)	6.17 (7.68)
	16QAM	5.97 (7.75)	9.31 (11.71)	6.62 (7.64)
	M=2 64QAM	6.13 (7.77)	10.34 (10.63)	6.71 (7.70)
LFDMA (OFDMA)	QPSK	5.16 (7.75)	8.93 (10.72)	5.67 (7.14)
	16QAM	5.22 (7.77)	8.63 (10.40)	5.72 (7.13)
	64QAM	5.49 (7.75)	8.51 (10.65)	5.85 (7.14)
IFDMA (OFDMA)	QPSK	3.87 (7.72)	8.02 (11.75)	5.19 (7.04)
	16QAM	5.19 (7.72)	9.18 (10.99)	5.67 (7.04)
	64QAM	5.47 (7.71)	9.43 (11.21)	5.80 (7.04)

TABLE II: Required power back-off to meet the given spectral mask for different MA schemes and different modulation schemes. In brackets, the respective power back-offs for the corresponding non-DFT precoded OFDMA schemes are given.

	QPSK	16QAM	64QAM
B-IFDMA, M=8	9.2 (10.7)	9.4 (10.7)	9.4 (10.7)
B-IFDMA, M=4	7.9 (9.3)	8.4 (9.3)	8.4 (9.3)
B-IFDMA, M=2	7.5 (9.0)	7.8 (9.0)	7.8 (9.0)
IFDMA	6.7 (8.5)	7.2 (8.5)	7.2 (8.5)

PAPR, respectively, than OFDMA. Moreover, both metrics indicate that the envelope fluctuations of OFDMA are independent of the modulation scheme. For higher order modulations such as 16QAM or 64QAM, IFDMA and LFDMA provide similar RCM and PAPR. For QPSK the RCM of LFDMA is ≈ 1.3 dB worse than for IFDMA whereas the average PAPR of LFDMA is ≈ 0.5 dB worse than for IFDMA. For B-IFDMA, both metrics indicate that the envelope fluctuations are significantly higher than for LFDMA and IFDMA. This effect is the more pronounced the higher the number of subcarriers per block. From Table I it can be also deduced that the maximum PAPR is not appropriate for evaluation of the envelope fluctuations because the probability of the peaks of the signal is very low.

In Fig. 5, the power spectral density (PSD) of an IFDMA signal at the amplifier output is shown. For modulation, QPSK is assumed. The Rapp-Parameter is chosen as $p = 2$, i.e., a non-linear power amplifier is assumed. The amplifier power back-off is chosen such that the PSD of the IFDMA signal meets the spectral mask. A realistic spectral mask, that is assumed throughout this work, can be found, e.g., in [22]. In Table II, the required power back-offs for IFDMA, B-IFDMA and the corresponding OFDMA schemes (in brackets) with different numbers of subcarriers per block are presented. They are obtained as exemplarily shown in Fig. 5 for IFDMA.

From Table II can be deduced that in case of B-IFDMA and IFDMA, for QPSK the required power back-off is slightly lower than for 16QAM and 64QAM, whereas for OFDMA the required power back-off is independent from the modulation scheme. For QPSK, the difference in the required back-off of the different B-IFDMA schemes and IFDMA is more pronounced

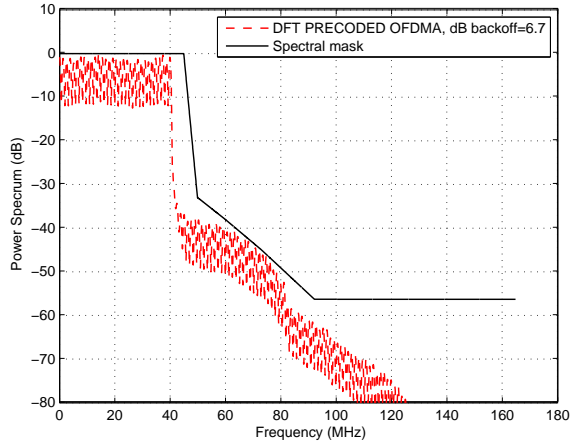


Fig. 5: PSD of an IFDMA signal at the amplifier output using QPSK modulation with a power back-off that is required to meet the given spectral mask.

TABLE III: Required E_s/N_0 in dB at a BER of 10^{-3} for IFDMA, LFDMA and B-IFDMA at different power back-offs for transmission over an AWGN channel.

back-off in dB	10	6	4	2	1	0
B-IFDMA, M=8	6.71	6.78	6.82	7.03	7.18	7.28
B-IFDMA, M=4	6.70	6.75	6.81	6.97	7.04	7.25
B-IFDMA, M=2	6.70	6.74	6.80	6.93	7.03	7.24
IFDMA	6.65	6.71	6.78	6.93	7.01	7.22
LFDMA	6.65	6.70	6.78	6.94	7.02	7.22

than for 16QAM and 64QAM.

For LFDMA, the spectrum assigned to a user is concentrated in a localized portion of the bandwidth. Consequently, the out-of-band radiation for LFDMA due to amplifier non-linearities is much smaller than for B-IFDMA and IFDMA. Thus, the PSD and the required power back-off to meet a spectral mask alone are not appropriate to evaluate the envelope fluctuations for LFDMA. In [23], filtering was only proposed for energy efficiency and works best with BPSK/QPSK.

In the following, the BER degradation due to the amplifier non-linearities is regarded. The parameters used are the same as for the previous investigations. In Fig. 6, the BER performance for IFDMA and the corresponding OFDMA scheme for QPSK modulation and transmission over an AWGN channel is shown dependent on the power back-off. A comparison of the results in Fig. 6 and in Table II shows that for the power back-off that is required to meet the spectral mask, the BER degradation is already negligible. Thus, the required power back-off in order to meet the spectral mask can be regarded as a more critical metric than the BER degradation. In Table III, the required E_s/N_0 for different power back-offs is compared for IFDMA, LFDMA and B-IFDMA. From Table III follows that for B-IFDMA, IFDMA and LFDMA respectively, a power back-off of ≈ 6 dB is required in order to provide only low BER degradations. Again, this value for the power back-off is lower than the required power back-off in order to meet the spectral mask.

Finally, in Fig. 7 the dependency of the different metrics is illustrated. On the x -axis, the required power back-off is given. On the y -axis, the corresponding values for the average PAPR and the RCM are given. In addition, again the required power back-off is depicted as a reference. From Fig. 7 follows that for low values for the required power back-off that correspond to IFDMA and B-IFDMA with 2 and 4 subcarriers per block the

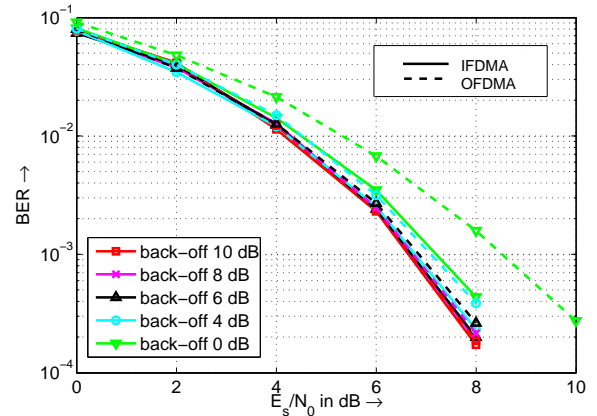


Fig. 6: BER performance of IFDMA and the corresponding non-DFT precoded OFDMA scheme with QPSK modulation for transmission using QPSK over an AWGN channel for different power back-offs.

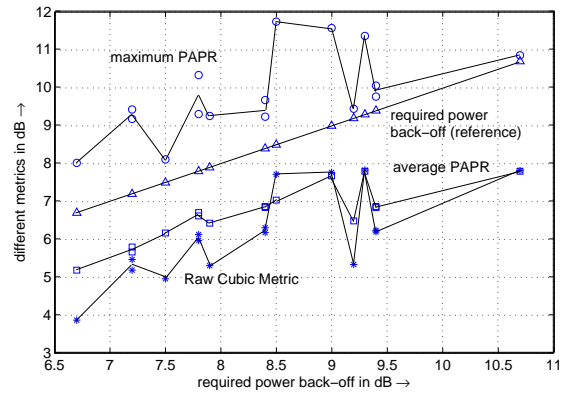


Fig. 7: Dependency between the metrics RCM, required power back-off to meet the given spectral mask, maximum PAPR and average PAPR.

average PAPR grows almost linearly with the required power back-off with a deviation of ≈ 1.5 dB. For the RCM and the maximum PAPR, the relation between the respective values and the required power-off is much more fluctuating dependent on the subcarrier allocation used. For required power back-offs larger than 9 dB corresponding to B-IFDMA with 8 subcarriers and the non-DFT precoded OFDMA schemes, the linear dependency between average PAPR and required power back-off is lost. As a conclusion, for B-IFDMA with up to 4 subcarriers per block as well as for IFDMA the required power back-off to meet the spectral mask can be easily estimated from the average PAPR, whereas for a higher number of subcarriers per block and for OFDMA this is not the case. Moreover, especially for B-IFDMA with up to 4 subcarriers per block and for IFDMA the average PAPR is more appropriate to estimate the required power back-off than the RCM or the maximum PAPR.

V. DESIGN OF THE PULSE SHAPING FILTER

Regarding Figs. 2 and 4, it can be concluded that oversampling and pulse shaping using an ideal lowpass filter significantly affects the good PAPR properties for IFDMA and B-IFDMA. Hence, the question arises if for these schemes it is possible to obtain lower envelope fluctuations by the choice of a different pulse shaping filter. In Fig. 8, the PSDs for IFDMA signals with different pulse shaping filters are shown. The corresponding average PAPR values of the IFDMA signals are given. From the results shown in Fig. 8 it can be concluded that there is a trade-off between low envelope fluctuations, low

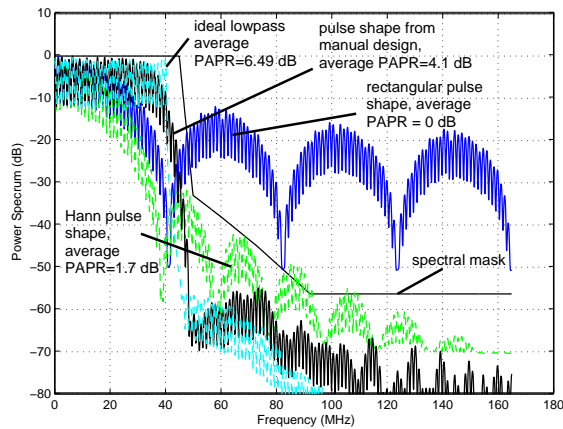


Fig. 8: PSD for an IFDMA signal before the amplifier for different pulse shaping filters and corresponding average PAPR for a bandwidth of 40 MHz.

out-of-band radiation and an efficient use of the band, i.e., a quasi rectangular PSD within the band. The lower the PAPR, the higher the out-of-band radiation and the more deviation of the main lobe of the PSD from the rectangular shape. Regarding these results it can be concluded that the ideal lowpass which is used throughout this work, cf., e.g., Fig. 5, already provides a good trade-off between efficient use of the spectrum, low out-of-band radiation and low envelope fluctuations. It provides an optimum use of the spectrum and low out-of-band radiation at the expense of acceptable envelope fluctuations.

VI. CONCLUSIONS

In this work, a novel signal model for oversampled, pulse shaped and windowed B-IFDMA is presented that includes the respective system models for IFDMA and LFDMA as special cases. The envelope fluctuations of DFT precoded OFDMA signals with different subcarrier allocation schemes are analyzed from different perspectives and using different metrics. New results for different metrics considering realistic transmit signals are presented and compared. The amplifier power back-off that is required to meet a spectral mask turns out to be a well suited metric in order to evaluate the envelope fluctuations for realistic systems. For the current investigation, as long as the signal is within the given spectral mask, the BER degradation at the receiver is negligible. As an exception, for LFDMA, where the signal of a user is concentrated in a localized portion of the bandwidth, the BER degradation at the receiver is a more critical metric. In general, the required power back-off can be determined regarding the PSD of a signal. For a running system, for IFDMA and B-IFDMA with a number of subcarriers per block up to 4, the required power back-off can be obtained from the average PAPR of the transmit signal, whereas for higher numbers of subcarriers per block and for non-DFT precoded OFDMA this is not the case. The CM and the maximum PAPR turn out to be not appropriate for estimation of the required power back-off due to the non-linear dependency between the respective values and the required power back-off. IFDMA and LFDMA provide similar average PAPR and CM values. Assuming realistic transmit signals, for B-IFDMA a higher power back-off is required compared to LFDMA and IFDMA. The power back-off increases with increasing number of subcarriers per block. Finally, an ideal lowpass filter in the DFT domain has been shown to be a good solution for the pulse shaping of an IFDMA or B-IFDMA signal because it provides an efficient use of the assigned bandwidth, low out-of-band radiation at the

expense of an acceptable increase of the envelope fluctuations which, nevertheless, provides still considerable power efficiency gains compared to non-DFT precoded OFDMA.

REFERENCES

- [1] WINNER, "Final report on identified RI key technologies, system concept, and their assessment," Tech. Rep. D2.10 v. 1.0, WINNER-2003-507581, December 2005.
- [2] H. Rohling, T. May, K. Brüninghaus, and R. Grünheid, "Broad-Band OFDM Radio Transmission for Multimedia Applications," *Proc. of the IEEE*, vol. 87, October 1999.
- [3] E. Costa and S. Pupolin, "M-QAM-OFDM System Performance in the Presence of a Nonlinear Power Amplifier and Phase Noise," *IEEE Trans. on Communications*, vol. 50, pp. 462–472, March 2002.
- [4] L. J. Cimini and N. R. Sollenberger, "Peak to Average Power Ratio Reduction of an OFDM Signal Using Partial Transmit Sequences," vol. 4, pp. 86–88, March 2000.
- [5] A. E. Jones and T. Wilkinson, "Combined Coding for Error Control and Increased Robustness to System Nonlinearities in OFDM," in *Proc. VTC96*, Atlanta, May 1996.
- [6] S. H. Müller and J.B. Huber, "OFDM with reduced peak-to-average power ratio by optimum combination of partial transmit sequences," vol. 33, pp. 368–369, February 1997.
- [7] B. S. Krongold and Jones D. L., "An active-set approach for OFDM PAR reduction via tone reservation," vol. 52, pp. 495–509, February 2004.
- [8] P. Xia, S. Zhou, and G. B. Giannakis, "Bandwidth- and Power-Efficient Multicarrier Multiple Access," *IEEE Trans. on Communications*, vol. 51, pp. 1828–1837, November 2003.
- [9] K. Brüninghaus and H. Rohling, "Multi-Carrier Spread Spectrum and its relation to Single-Carrier Transmission," in *Proc. IEEE Vehicular Technology Conference*, Ottawa, Ontario, Canada, May 1998, pp. 2329–2332.
- [10] U. Sorger, I. De Broeck, and M. Schnell, "IFDMA - A New Spread-Spectrum Multiple-Access Scheme," in *Proc. ICC'98*, Atlanta, Georgia, USA, June 1998, pp. 1013–1017.
- [11] T. Frank, A. Klein, E. Costa, and E. Schulz, "IFDMA - A Promising Multiple Access Scheme for Future Mobile Radio Systems," in *Proc. PIMRC 2005*, Berlin, Germany, Sep. 2005.
- [12] T. Frank, A. Klein, and Costa, "An Efficient Implementation for Block-IFDMA," in *Proc. PIMRC 2007*, Athens, Greece, Sep. 2007.
- [13] 3GPP TSG RAN, "Physical Layer Aspects for Evolved UTRA (Release 7)," TR 25.814v1.5.0, 3rd Generation Partnership Project, Technical Specification Group, Sophia-Antipolis, France, 2006.
- [14] H. G. Myung, J. Lim, and D. J. Goodman, "Peak-to-Average Power Ratio of Single Carrier FDMA Signals with Pulse Shaping," in *Proc. of PIMRC06*, Helsinki, Finland, September 2006.
- [15] T. Svensson et al., "B-IFDMA - A Power Efficient Multiple Access Scheme for Non-frequency-adaptive Transmission," in *Proc. of 16th Mobile & Wireless Communications Summit*, Budapest, Hungary, July 2007.
- [16] TSG RAN WG4 31 3GPP, TDoc R4-040367, "Comparison of PAR and Cubic Metric for Power-Derating," Tech. doc., 2004.
- [17] D. Falconer, F. Danilo-Lemaine, C.-T. Lam, and M. Sabbaghian, "Power Backoff Reduction for Generalized Multicarrier Waveforms," in *Proc. EUSIPCO07*, Poznan, Poland, September 2007, pp. 693–697.
- [18] T. Behravan, A. Eriksson, "Bandpass Compensation Techniques for Bandpass Nonlinearities," in *Proc. VTC03*, Orlando, Florida, USA, October 2003.
- [19] T. Frank, A. Klein, E. Costa, and E. Schulz, "Interleaved Orthogonal Frequency Division Multiple Access with Variable Data Rates," in *Proc. International OFDM Workshop 2005*, Hamburg, Germany, Aug./Sep. 2005, pp. 179–183.
- [20] R. van Nee and Ramjee Prasad, *OFDM for Wireless Multimedia Communications*, Artech House, 1st edition, 2000.
- [21] A. Skrzypczak, P. Siohan, and J.-P. Javardin, "Power Spectral Density and Cubic Metric for the OFDM/OQAM Modulation," in *Proc. of ISSPIT2006*, 2006, pp. 846–850.
- [22] WINNER, "The WINNER II Air Interface: Refined multiple access concepts," Tech. Rep. D4.6.1, IST-4-027756 WINNER II, November 2006.
- [23] H. Wu and T. Haustein, "Energy and Spectrum Efficient Transmission Modes for the 3GPP-LTE Uplink," in *Proc. of PIMRC07*, Athens, Greece, September 2007.